

Terahertz Pulsed Spectroscopy as a New Tool for Measuring the Structuring Effect of Solutes on Water

N. KAUN, J. R. BAENA, D. NEWNHAM, and B. LENDL*

Institute of Chemical Technologies and Analytics, Vienna University of Technology, Getreidemarkt 9-164, 1060 Vienna, Austria (N.K., J.R.B., B.L.); and TeraView Limited, Platinum Building, St John's Innovation Park, Cambridge CB4 0WS, UK (D.N.)

Absorption spectra of aqueous solution of “chaotropes” (structure maker) and “kosmotropes” (structure breaker) have been recorded in the mid-infrared (MIR) and terahertz (THz) spectral region. A different impact of the two groups of solutes on the absorption spectrum of water was found in the recorded THz spectra. A concentration-dependent increased absorption across the investigated THz spectral region (0.04–2 THz, 1.3–66 cm⁻¹, respectively) has been recorded for all studied chaotropic solutions, whereas the opposite has been obtained for kosmotrope containing solutions. In the case of ionic solutes a further increase in absorption towards higher frequencies was measured. The distinction between chaotrope and kosmotrope solutes was, as expected, also possible in the MIR spectral region. Depending on the structure-forming effect of the solute the OH stretch vibration of the water (around 3400 cm⁻¹) was slightly shifted. A red shift has been observed for solution of kosmotropes, whereas a blue shift was observed in the case of solutions containing chaotropes. Compared to the MIR spectral region the structure influencing effect of solutes can be more efficiently studied in the THz spectral region, which provides information from interactions between neighboring water molecules.

Index Headings: Terahertz pulsed spectroscopy; Aqueous solution; Water structure.

INTRODUCTION

Significant instrumental developments over the last decades have established spectroscopic techniques from the ultraviolet regions down to the far-infrared spectral region as powerful, often indispensable tools in modern chemical research. In the near (NIR) and mid-infrared (MIR) spectral region a range of experiments in water and aqueous solution are possible today that were considered impossible only some years ago. Two selected examples underpin this statement: determination of secondary structures of proteins in aqueous solution¹ and following the action of single amino acids with nanosecond time resolution in protein reactions.² These experiments are now possible using commercially available bench top instruments that can be found in many research and routine laboratories. Significantly less use is made of the far-infrared spectral region due to reduced instrument performance when thermal light sources and photon detectors are employed as in their popular counterparts for the NIR and MIR spectral regions. When moving to the even longer wavelengths of the terahertz (THz) spectral region, few reports on the use of a broadband spectrometer can be found in the literature. This is explained by the poor brightness of thermal light sources and by additional experimental difficulties as this spectral region

covers frequencies too high to be accessible by electronics and too low for photonic devices.³ However, this situation is about to change as new instrumentation becomes available to the interested chemists who want to explore this still unused spectral region. Among these new possibilities, THz measurement capabilities at synchrotron beamlines across the world^{4,5} must be mentioned along with a recently available dedicated portable terahertz pulsed spectrometer that covers a frequency from 0.04 to 4 THz, which corresponds to the spectral region from 1.3–133 cm⁻¹ or 8 mm to 75 μm wavelength. A terahertz pulsed spectrometer uses low power, ultra-short pulses of broadband electromagnetic radiation at lower frequencies than traditional infrared techniques.⁶ The technology uses fs-pulse lasers, which are focused onto a semiconductor, resulting in the emission of a pulse of coherent terahertz radiation. The radiation is detected using a solid-state room-temperature receiver.⁷ Very high signal-to-noise ratios (>10⁵) can be achieved using optical gating. As the technique is coherent both electric-field amplitude and phase information can be measured at the same time, from which the spectral absorption coefficients, $\alpha(\omega)$, and the refractive indices, $n(\omega)$, of the material can be directly extracted.

Terahertz spectroscopy has already found application in imaging instruments, which have been set up recently with great success providing pictures of biological samples with complex structure such as tissue and dry biological cells.^{8,9} Furthermore, using sophisticated time domain experiments, physicists have used THz spectroscopy to gain information on fast dynamic systems to extract, for example, the dielectric constants of water as a function of temperature.¹⁰

To explore this spectral region for (bio)chemical research, fundamental investigation on the spectral properties of aqueous solution are needed. In this contribution we report on THz spectra of selected solutes at different concentrations. The data obtained strongly suggest that THz spectroscopy provides a direct means to observe structure-forming effects of the solutes on water. For water, two distinct bands are found in the THz region: the nominal 60 and 180 cm⁻¹ intermolecular vibrations.¹¹ In general intermolecular interactions from the hydrogen-bonded network of water are to be expected down to two wavenumbers.¹²

The structure of water is a very complicated topic and descriptions have been attempted through many different models. Stanley and Teixeira¹³ have put these models into two categories: mixture/interstitial models and distorted hydrogen bond models (continuum models). In the mixture/interstitial model, properties of water can be de-

Received 10 August 2004; accepted 30 November 2004.

* Author to whom correspondence should be sent. E-mail: Bernhard.lendl@tuwien.ac.at.

scribed by a mixture of distinct species of water molecules in certain equilibrium. These species can be identified by a defined number of hydrogen bonds that are interacting.¹⁴ In the continuum model, water is assumed to form a network that is more or less completely hydrogen bonded. Their effort to combine these models has led to the “percolation model”.¹³ To understand the influence of a dissolving substance on the structure of liquid water other models more focused on this topic are preferred. In general, solutes can be classified in to two groups: the “kosmotropes” (order makers) and the “chaotropes” (disorder makers).¹⁵ This effect can now be described by, e.g., the increase or decrease of viscosity due to the addition of a solute, which is done well as a basis for simulation in Hribar et al.¹⁶ In a similar way, the influence on the water structure is given by the entropy of water near monovalent ions (ΔS_{II}) as calculated from the entropy of hydration of the ion.¹⁷ The ΔS_{II} serves as a measure for the tightness of the bonding of the dissolved ions and water. The solute either strengthens or weakens the water–water interactions and therefore water becomes more or less mobile. In other work,^{18,19} the structure of water is given by a root mean square (rms) of the bimodal H-bond angle distribution, made up of nearly linear bonds and stronger bent O···O–H bonds. Adding a solute can increase or decrease the rms value, indicating either more or less distorted water bonds. Rønne and Keiding¹⁴ propose equilibrium between a low-density liquid (LDL) with high local tetrahedral ordering similar to ice and a high-density liquid with less connected water molecules.

Mid-infrared spectroscopy is sensitive to changes in hydrogen bonding. These changes are generally reflected in a decrease in frequency of the respective vibrations. Therefore, a shift in the position of the ν -OH of the water molecule may be expected, if the extent and modes of hydrogen bonding in water are affected by the presence of kosmotropes or chaotropes. This has been observed and exploited already by various groups,^{18,19,21} who described the ν -OH band at 3400 cm^{-1} as a convolution of several OH stretch vibrations corresponding to water species interacting with each other via hydrogen bonding to a varying extent. For simplicity, two extreme cases, “ice-like”, characterized by a high degree of hydrogen bonding and a ν -OH at wavenumbers lower than 3400 cm^{-1} , and “free” water that is more similar to water in the vapor phase with minimum hydrogen bonding and a corresponding ν -OH peak maximum at wavenumbers higher than 3400 cm^{-1} , have been defined.²¹ For discussing the water spectra in the THz spectral region, where we expect to see intermolecular interactions, we will use this simplistic view of the water structure, sticking to the terms “ice-like” and “free” water.

Adding a kosmotrope (an order maker) shifts the equilibrium to the “ice-like” side, which means that the order is increasing. Vice versa, adding chaotropes increases the amount of “free” water. Typical kosmotropes are small or multiple charged ions (e.g., SO_4^{2-} , Li^+ , Na^+) as well as non-ionic kosmotropes like trehalose or sucrose. In general, these ions/molecules are highly hydrated and therefore affect the dynamics of water molecules in their neighborhood by the presence of hydration layers, hindering mobility. Representative chaotropes are large single charged ions with low charge density (e.g., Gdm^+ ,

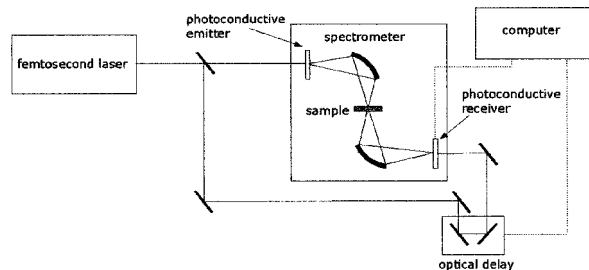


FIG. 1. Schematic showing the configuration of the TPI[®] spectra 1000 (TeraView Limited).

SCN^- , Cl^-). Their tendency to bind to water is weaker than the tendency of water to bind to itself. As a consequence, the water adjacent to the ion/molecule becomes more mobile than bulk water (i.e., weakly held). It is very important to consider that the strength of both effects is dependent on the concentration of the solute. Furthermore, ionic kosmotropes should be treated differently from non-ionic kosmotropes. The hydration shell of ionic kosmotropes is characterized by a directed and polarized arrangement of the surrounding water molecules.

EXPERIMENTAL

For this study, HPLC grade water from Sigma-Aldrich was used. Trehalose, potassium thiocyanate, magnesium sulfate, and guanidium chloride (GdmCl) were purchased from Fluka, and ammonium nitrate and sodium chloride were purchased from Merck. Solutions in concentrations ranging from 0.01 M to 1 M were prepared.

Spectra of water in the MIR spectral region were recorded on capillary films between two CaF_2 windows on a Bruker Equinox 55 at $22\text{ }^\circ\text{C}$ equipped with a Globar source and a liquid nitrogen cooled mercury cadmium telluride (MCT) detector. The spectral resolution was set to 4 cm^{-1} . All measurements and calculations were checked for reproducibility.

The terahertz measurements were made in transmission using a TPI[®] spectra 1000 spectrometer (TeraView Limited, Cambridge, UK). Spectra were the average of 1800 scans (approximately 1 min measuring time). Data were acquired using OPUS[®] software (Bruker Optics, Germany). A schematic diagram of the experimental setup for a terahertz pulsed spectrometer system is shown in Fig. 1. Terahertz pulses are generated when ultra-short laser pulses, from a 75 fs bandwidth-limited titanium–sapphire laser (Vitesse, Coherent, US) operating at 800 nm with a repetition rate of 80 MHz, are focused onto a gallium arsenide (GaAs) photoconductive switch, the terahertz emitter. When the ultra-short laser pulse is present photocarriers are generated in the switch; a transient current flows across a dipole antenna giving rise to a short burst of broadband terahertz radiation. A hemispherical silicon lens couples the radiation out of the GaAs substrate into free-space. Parabolic mirrors focus the terahertz radiation onto the sample. Detection of the terahertz radiation is achieved using an optically gated semiconductor receiver antenna similar to the emitter. The femtosecond near-infrared laser pulses optically gate the switch. The time delay between the terahertz and optical pulses is varied to measure a representation of the terahertz

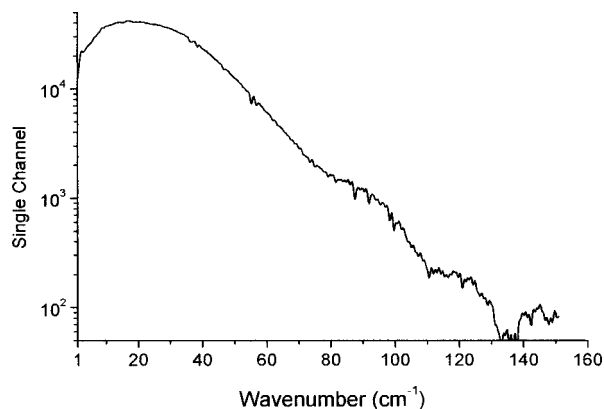


FIG. 2. Single beam spectrum of the empty cell compartment.

hertz field. Fourier-transforming the resultant time-domain waveform provides the frequency information.

For terahertz measurements a standard flow cell, as used for MIR spectroscopy, was equipped with two polyethylene (PE) windows of 4 mm thickness and a 50 μm spacer and installed in the N_2 purged sample compartment. The cell was connected via Teflon tubing to a peristaltic pump, which was operated at a low flow rate of 0.5 mL/min. Spectra were acquired with the flow on. The procedure was to start with the lowest concentration of a solute, then move on to examining the next higher one. A baseline shift, especially towards the end of the scale during a measurement campaign of several hours, has to be considered for the current instrument performance. Therefore, after each series, a water spectrum for a new background was recorded. The instrument allowed us to acquire spectra from 1 to 133 cm^{-1} employing a spectral resolution of approximately 1 cm^{-1} . Figure 2 shows a single beam terahertz spectrum with the empty flow cell. It reveals that there is detectible signal from 1 cm^{-1} until 133 cm^{-1} . However, in the experiments reported here, the low signal above 60 cm^{-1} can lead to reproducibility problems. Therefore, we focused on the region from 1 to 60 cm^{-1} that provided acceptable baseline stability and noise factor (rms error of deviation in absorbance upon repeated measurement) of less than 10^{-3} a.u. in water for 1800 scans.

RESULTS

Mid-infrared Spectra of the Prepared Solutions. Information about the water structure is collected in a common way by recording absorbance spectra from 2950 cm^{-1} to 3700 cm^{-1} for the six different water solutions and pure water versus the empty cell; this information is presented in Fig. 3. The spectra have been normalized to the maximum of their $\nu\text{-OH}$ band absorption. The appearance of the $\nu\text{-OH}$ band results from a contribution of all water structures existing in the probed liquid. A clear variation in shape of this band and a shift in the position of the peak maximum of the solutions compared to the HPLC grade water can be observed. Taking into account that each different water structure present in the sample contributes to this peak at other frequencies, it becomes clear that we can observe the influence of the various added solutes on water. In the work of Brubach et al.,²¹ a decomposition of the feature into three peaks has been

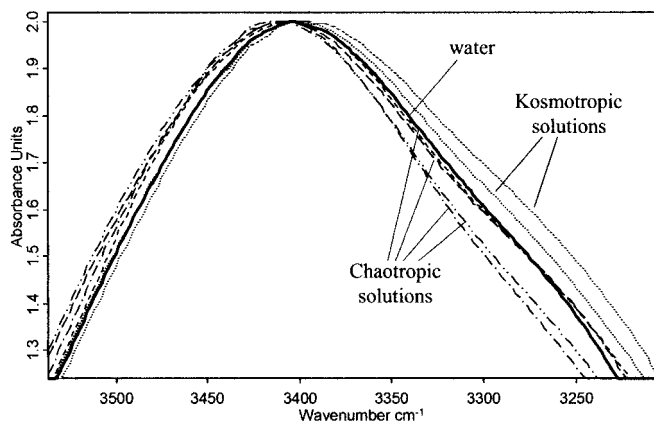


FIG. 3. Spectra of six different solutions. The dotted lines give the kosmotropes trehalose (0.5 M) and MgSO_4 (1 M). The dashed lines are the KSCN (0.5 M), GdmCl (0.5 M), NH_4NO_3 (1 M), and NaCl (1 M). The solid line refers to HPLC grade water.

carried out. The first peak at $\sim 3310 \text{ cm}^{-1}$ can be assigned to “ice-like” water molecules, the second ($\sim 3440 \text{ cm}^{-1}$) to intermediate water molecules, and the third ($\sim 3570 \text{ cm}^{-1}$) to multimer water molecules, which means going from more “ice-like” structure to “free” water similar to the vapor phase. From our measurements, it can be stated that trehalose and MgSO_4 solutions have larger contributions from the more “ordered” water than the “free” water. This observation is consistent with the theory that considers them kosmotropes. On the other hand, KSCN, GdmCl, NH_4NO_3 , and NaCl show a slightly increased absorbance in the higher wavenumber region and are therefore considered to be chaotropes.

Recorded Terahertz Spectra. Figure 4 presents an absorbance spectrum of the dry flow cell with the empty cell compartment as background. A dominant band at 72 cm^{-1} is assigned to the polyethylene window material used.²² In Fig. 5 an absorbance spectrum of water with the empty (air filled) flow cell as background is shown. In the THz region generally two vibrational modes for water are found, centered at approximately 60 and 180 cm^{-1} . The one band at 60 cm^{-1} accessed by these measurements is weak in absorption spectroscopy (in contrast to Raman spectroscopy) and even diminishes for temperatures higher than 0 $^\circ\text{C}$.²³ With the current instrument performance the band is hardly discernible from baseline

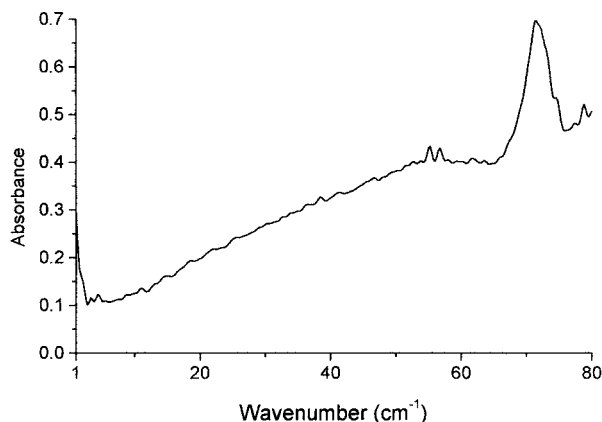


FIG. 4. Absorbance spectrum of the empty flow cell containing PE windows.

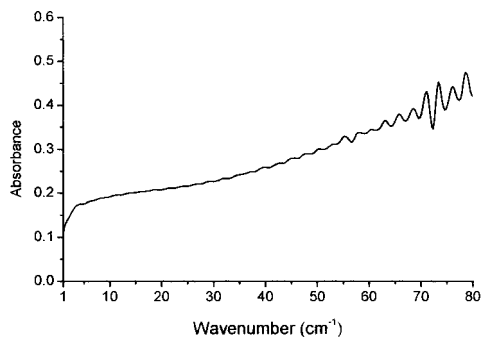


FIG. 5. Spectrum of pure water against the empty cell.

noise. The obtained spectrum, however, is in good agreement with measured literature data.²⁴

The influence of various solutes on the absorbance of water in the THz region was studied first by two sets of typical chaotropes in solution and two sets of kosmotropes, each set consisting of various concentrations from 0.01 M up to 1 M. Figure 6 presents the results as absorbance spectra against water. Although no bands of the dissolved solutes could be observed, very interesting changes in the intensity of the water background could be detected.

The ions K^+ and SCN^- , both large ions, form a typical chaotropic substance. SCN^- in its linear structure has special hydration properties and is known as an extremely weak hydrated ion.²⁵ The second tested chaotrope is formed by Gdm^+ and Cl^- . Guanidinium is known as one of the most weakly hydrated cations.²⁵ Both sets of solutions give an overall increase in absorption.

The other two dissolved salts are $MgSO_4$, which be-

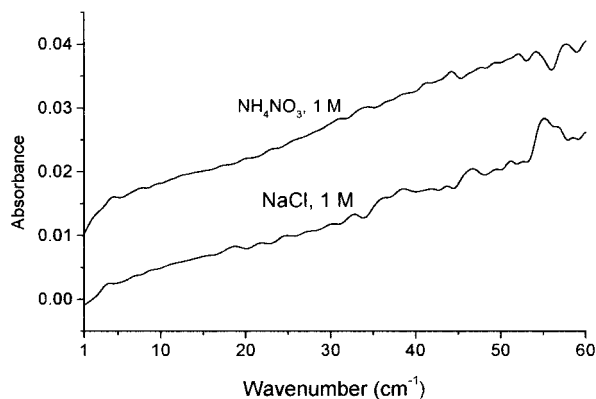
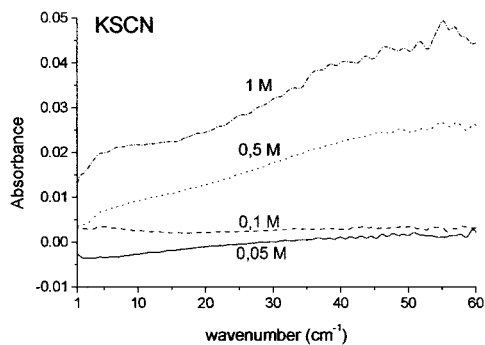


FIG. 7. Absorbance spectra with H_2O spectra as background of 1 M NH_4NO_3 , which is expected to be a chaotrope, and $NaCl$ of uncertain character.

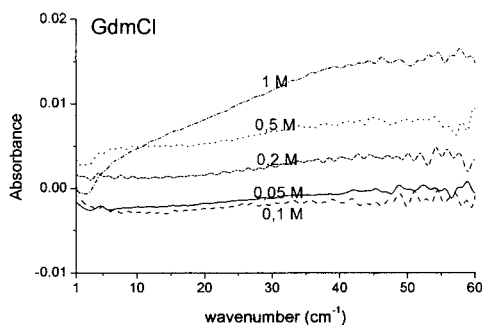
longs to the group of kosmotropes, due to the high charge densities of its ions, and trehalose, a special kosmotrope.^{15,26} The spectra in Figs. 6c and 6d show a clear decrease in absorption.

A further substance, NH_4NO_3 , which is categorized as a chaotrope,¹⁵ is measured as 1 M concentrated solution. Indeed, the spectrum also shows increased absorption (Fig. 7). A check for $NaCl$ was carried out, where the Na^+ ion actually is considered marginally as a kosmotropic ion and Cl^- , on the other hand, as a weak chaotrope.^{17,24} Figure 7 shows that the influence of a 1 M concentrated $NaCl$ solution on the water leads to an increase in absorbance.

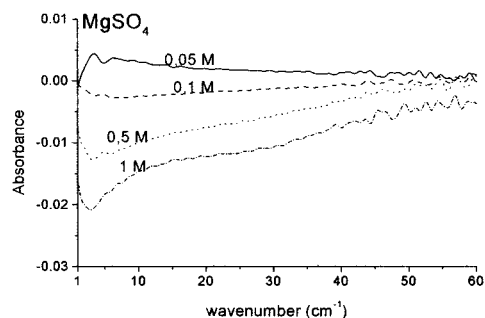
In general, the lowest concentrations (0.05 M and 0.1 M) do not show a distinct change in absorption compared



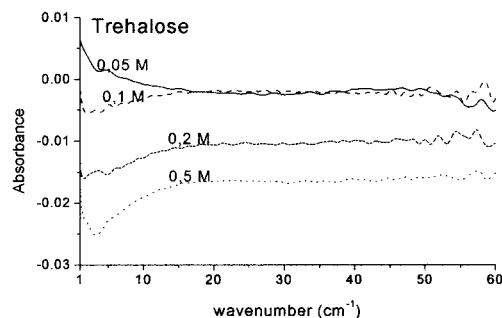
a)



b)



c)



d)

FIG. 6. Absorbance spectra of representative chaotropes (a) $KSCN$ and (b) $GdmCl$ and kosmotropes (c) $MgSO_4$ and (d) trehalose against pure water.

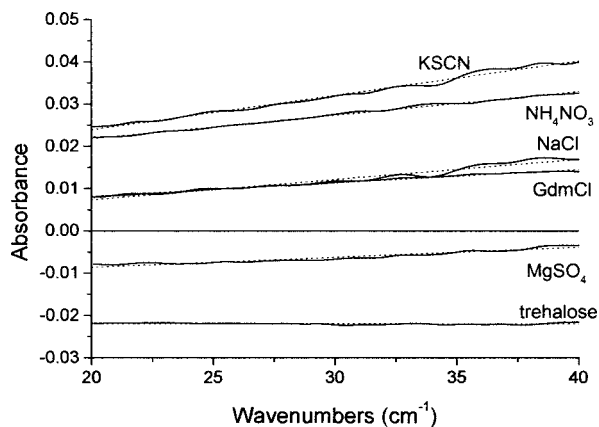


FIG. 8. Recorded absorbance spectra with H₂O spectra as background and linear fit of the spectra obtained from the highest measured concentration in the region from 20 to 40 cm⁻¹. The corresponding equation factors are presented in Table I.

to water. However, the observed shifts upwards or downwards for higher concentrations differ in their behavior from each other and also in absorption intensities. While in most cases a shift in absorbance also results in an ascending slope, the solute trehalose does not show this tendency and also the GdmCl gives a very weakly pronounced slope.

For better comparison, the slopes of the curves of the 1 M concentrated solutions (0.5 M for the trehalose) were calculated according to the formula $y = m \cdot x + b$ for the region between 20 and 40 cm⁻¹, where we observed the best reproducibility, in order to tabulate this observation (Fig. 8). The obtained values for the linear fit are presented in Table I, where the calculated slopes (m) and the ordinates (b) corresponding to the measured absorbance spectra in the spectral region from 20 to 40 cm⁻¹ of the solutes 1 M and 0.5 M, respectively, are given.

DISCUSSION

The chosen solutes, as chaotropes or kosmotropes respectively, yield the expected results in the IR: more “ice-like” water structure for the kosmotropes, more “free water” for the latter. Nevertheless, these variations are marginal and attempts to analyze the difference in a systematic way by peak fitting failed due to ambiguous results. One reason is the influence of drifts in the baseline. As a consequence, the OH band provides a hint, more than an absolute measure, for assigning the influence of a solute in a certain concentration to one or the other effect. This has also been commented on by Brubach et al.²⁷

In the studied THz region (1.3 cm⁻¹ to 60 cm⁻¹ wavenumber/8 mm to 160 μm wavelength), no peaks of water could be found at room temperature. Also, the solutes did not give any vibrational bands. However, correlating with the results from the MIR, changes in absorption intensities with respect to pure water are observed as an overall increase or decrease in the THz region.

Within this work it was not possible to unravel the exact mechanism causing these shifts, but a direct relation to structural changes of water can be stated. The observed effect of shifting absorbance spectra cannot be explained by varying water concentration due to the presence of

TABLE I. Values for the linear fit of Fig. 8.

	Slope (m)	Intercept (b)
MgSO ₄	2.4×10^{-4}	-1.3×10^{-2}
trehalose	2.5×10^{-6}	-2.1×10^{-2}
KSCN	8.2×10^{-4}	7.6×10^{-3}
GdmCl	3.2×10^{-4}	1.9×10^{-3}
NH ₄ NO ₃	5.6×10^{-4}	1.1×10^{-2}
NaCl	4.8×10^{-4}	-2.3×10^{-3}

solutes. In order to cause such strong variation by density changes, the concentration of water in solution would have to de- or increase up to 5%, which is not the case.

A more likely explanation for the measured spectra changes is the rotational dynamics due to the alteration of the water structure due to the presence of the solutes.

The measured spectra allow a differentiation between a kosmotropic and a chaotropic behavior of solutes in water, especially when their concentration is high enough, around 0.2 M.

This is given by an overall increase or decrease in absorption with respect to pure water. The value of b presented in Table I was found to be a discriminator for chaotropic and kosmotropic effects, but due to the instrument instability in the baseline one should still consider this cautiously. NH₄NO₃, consisting of two large ions, was in good agreement with theory and its b value was in the range of the other chaotropes. However, NaCl, stated in literature¹⁷ as more or less neutral to the kosmotropic/chaotropic effect, showed a gain in absorption. NaCl consists of the weak kosmotrope Na⁺ and the weak chaotrope Cl⁻. Looking at the value of b , it is seen that the value is conspicuously lower than from the other chaotropic salts. Probably it is only due to the slope that NaCl shows such a strong shift up. The comparison of the m values in Table I confirms the following consideration: all ionic substances show a value in the same range, while trehalose, revealing an almost flat line similar to a uniform baseline shift, gives a value two orders of magnitude lower. Furthermore, the slope is increasing with the concentration, independently of whether a movement downwards or upwards is observed. The observed result may be explained by two superposed effects. On one hand there is the overall shift in intensity, which can be directly related to the ability of the solutes to force water into certain structures (kosmotropic/chaotropic behavior). On the other hand, the value of the slope may be used to differentiate ionic from non-ionic solutes. This value is thus most likely correlated to the conductivity of the solutions.

However, at this point we cannot exclude the possibility that there is an influence from the vibrational bands from higher energy on the spectral region below 60 cm⁻¹. It can be ruled out from overview spectra that the librational band at 600 cm⁻¹ does contribute to this region, but an impact from the intermolecular vibration at 180 cm⁻¹ on the lower wavenumber region may be possible.

CONCLUSION

The THz spectra of aqueous solution of different solutes can thus be viewed as a combination of two different effects that are reflected in the slope and intercept of the simplified spectrum, respectively. We propose that from

the sign of the intercept (positive or negative) a distinction between chaotrope and kosmotrope can be made. A significant slope is only observed for ionic substances. Salts whose kosmotrope or chaotrope behavior is under discussion in the literature also give rise to unclear results so far. However, these first results using recently available terahertz pulsed spectrometers are highly promising in light of improvements in instrument stability and thus signal-to-noise ratio, which most likely can be expected in the near future, and merit further investigation.

ACKNOWLEDGMENT

N.K., J.R.B., and B.L. are grateful for financial support received from the Austrian Science Fund within the project FWF 15531. J.R.B. also acknowledges support from the Consejería de Educación y Ciencia de la Junta de Andalucía.

1. H. Fabian and W. Mäntele, "Infrared Spectroscopy of Proteins", in *Handbook of Vibrational Spectroscopy*, J. M. Chalmers and P. R. Griffiths, Eds. (John Wiley and Sons, Ltd., Chichester, 2002), pp. 3399–3425.
2. K. Gerwert, *Biol. Chem.* **380**, 931 (1999).
3. M. F. Kimmitt, *J. Biol. Phys.* **29**, 77 (2003).
4. L. M. Miller, G. D. Smith, and G. L. Carr, *J. Biol. Phys.* **29**, 219 (2003).
5. M. Abo-Bakr, K. Feikes, K. Hollmack, P. Kuske, W. B. Peatman, U. Schade, G. Wustefeld, and H.-W. Hübers, *Phys. Rev. Lett.* **90**, 094801/1 (2003).
6. P. F. Taday, I. V. Bradley, D. D. Arnone, and M. Pepper, *J. Pharm. Sci.* **92**, 831 (2002).
7. C. Fattinger and D. Grischkowsky, *Appl. Phys. Lett.* **54**, 490 (2002).
8. V. P. Wallace, P. F. Taday, A. J. Fitzgerald, R. M. Woodward, J. Cluff, R. J. Pye, and D. D. Arnone, *Faraday Discuss.* **126**, 255 (2003).
9. U. Schade, K. Hollmack, P. Kuske, G. Wustefeld, and H.-W. Hübers, *Appl. Phys. Lett.* **84**, 1422 (2004).
10. C. Rønne, P. Åstrand, and S. R. Keiding, *Phys. Rev. Lett.* **82**, 2888 (1999).
11. G. E. Walrafen, Y. C. Chu, and G. J. Piermarini, *J. Phys. Chem.* **100**, 10363 (1996).
12. L. Thrane, R. H. Jacobsen, P. U. Jepsen, and S. R. Keiding, *Chem. Phys. Lett.* **240**, 330 (1995).
13. H. E. Stanley and J. Teixeira, *J. Chem. Phys.* **73**, 3404 (1980).
14. C. Rønne and S. R. Keiding, *J. Mol. Liq.* **101**, 199 (2002).
15. <http://www.lsbu.ac.uk/water/kosmos.html>.
16. B. Hribar, N. T. Southall, V. Vlachy, and K. A. Dill, *J. Am. Chem. Soc.* **124**, 12302 (2002).
17. K. D. Collins, *Proc. Natl. Acad. Sci., U.S.A.* **92**, 5553 (1995).
18. K. A. Sharp, B. Madan, E. Manas, and J. M. Vanderkooi, *J. Chem. Phys.* **114**, 1791 (2001).
19. F. Vanzi and B. Madan, and K. J. Sharp, *Am. Chem. Soc.* **120**, 10748 (1998).
20. R. Laenen, C. Rauscher, and A. Laubereau, *J. Phys. Chem. B* **102**, 9304 (1998).
21. J. B. Brubach, A. Mermet, A. Filabozzi, A. Gerschel, D. Lairez, M. P. Krafft, and P. Roy, *J. Phys. Chem. B* **105**, 430 (2001).
22. T. Tanabe, K. Suto, J. Nishizawa, K. Saito, and T. Kimura, *J. Phys. D: Appl. Phys.* **36**, 953 (2003).
23. O. F. Nielsen, *Annu. Rep. Prog. Chem., C: Phys. Chem.* **93**, 57 (1997).
24. E. Zoidis, J. Yarwood, and M. Besnard, *J. Phys. Chem. A* **1003**, 220 (1999).
25. P. E. Mason, G. W. Neilson, C. E. Dempsey, A. C. Barnes, and J. M. Cruickshank, *Proc. Natl. Acad. Sci., U.S.A.* **100**, 4557 (2003).
26. C. Branca, S. Magazu, G. Maisona, S. M. Bennington, and B. Fak, *J. Phys. Chem. B* **107**, 1444 (2002).
27. J. B. Brubach, A. Mermet, G. de Marzi, C. Bourgaux, E. Prouzet, and P. Roy, *J. Phys. Chem. B* **106**, 1032 (2002).